ELSEVIER

Journal of Materials Processing Technology 136 (2003) 146–150

Journal of Materials Processing Technology

www.elsevier.com/locate/jmatprotec

Study of shrinkage strains in a stereolithography cured acrylic photopolymer resin

D. Karalekas*, A. Aggelopoulos

Department of Technology & Production Systems, University of Piraeus, Karaoli & Dimitriou 80, 185 34 Piraeus, Greece

Received 13 October 2000; received in revised form 19 July 2002; accepted 12 November 2002

Abstract

The shrinkage characteristics of stereolithography (SL) built square laminate plates using an acrylic-based photopolymer were studied after they had been post-cured under ultraviolet and thermal exposure. The specimen plates consisted of a resin layer laser cured on an identical layer of the same material that had already been cured and post-cured. The assembled laminate was then cured, and the resulting out-of-plane displacement (warpage) due to shrinkage was recorded by means of the shadow moiré method. The exhibited warpage of the plates was related to the polymerisation shrinkage strains through the elastic lamination theory, which was implemented to calculate the magnitude of the resulting shrinkage strains. It was obtained that the acrylic-based resin plates exhibited considerable warpage, while thermal post-curing resulted to higher shrinkage in the *y*-axis of the plates.

Keywords: Photopolymer; Shrinkage; Stereolithography; Projection moiré; Warpage

1. Introduction

Stereolithography (SL) nowadays is one of the most common rapid prototyping techniques used for product development purposes, where the part accuracy is a direct result of the properties of the materials used. The most commonly used materials for fabrication of rapid prototypes by laser solidification (SL technique) are photopolymer resin systems experiencing shrinkage upon changing from liquid to solid during laser curing. This results in stress and subsequently in strain deformations leading to considerable curl distortion. Residual stresses in SL formed parts are a direct consequence of the shrinkage of the polymeric material during curing. Residual stresses generated during part building may be responsible for creep distortions, which occur long after the part is built, or cause cracks and delamination within the part [1]. The distortion caused by shrinkage during polymerisation and the layer-by-layer building process is considered to be an important shortcoming in SL.

The curing process of resins involves several phase changes as a result of thermal and chemical mechanisms. It is usual to distinguish between the chemical and thermal components of shrinkage [2]. Chemical or polymerisation shrinkage occurs during crosslinking of the polymeric system and depends on the chemical composition and polymerisation reaction. Its level depends on the polymer glass transition temperature, T_g, the curing temperature as well as on the exposure amount and rate.

Various studies have been undertaken to investigate the curing of photopolymers used in the SL process and the mechanisms of the resulting shrinkage. Curing (both heat and UV initiated) characteristics of an acrylic-based photopolymer under actual fabrication conditions were studied using Raman spectroscopy as well as differential scanning calorimetry (DSC) and differential scanning photo-calorimetry (DSP) [3,4]. Dusel et al. [5] have presented results showing the course of shrinkage, force and temperature of a 0.4 mm deep polymerised slab over time for a hybrid resin system. Chemical shrinkage of resins has been measured by casting the resin on an aluminium beam and measuring strains in that beam during curing [6]. This technique requires embedding of resin gauges between the aluminium and the resin beams and compensation for thermal effects.

The aim of the work presented here, was to determine the magnitude of the shrinkage strains resulting during the polymerisation of a typical SL photopolymer by conducting a series of simple and direct experiments. The followed methodology is based on measuring the warpage of SL cured

* Corresponding author.

0924-0136/03/$ – see front matter
doi:10.1016/S0924-0136(03)00028-1

and post-treated resin plates and then using the elastic lamination theory to calculate the resultant polymerisation shrinkage strains. This method was first developed by Daniel and co-workers [7,8] and used to obtain the chemical cure shrinkage in epoxy matrix laminates.

2. Experimental procedure

The resin material investigated was an acrylic-based photopolymer (Allied Signal Exactomer 2202 SF). An EOS stereos desktop SL system using a UV laser beam was employed for the fabrication of the test specimens. Thin liquid resin layers of 0.156 mm thickness were laser cured (all layers were scanned in the same direction) during the SL layer-by-layer building process to form square laminate plates (10 cm × 10 cm × 3.3 cm). Then, the plates were fully polymerised (post-cured) by placing half of them in a UV chamber for 8 h and the remaining ones in an oven at 80 °C for the same length of time. One surface of the post-treated plates was sanded lightly and coated with a thin layer of primer to help the adhesion of the second resin layer to it.

A second layer of the same material, thickness and laser scan orientation was stacked on top of the initially fully cured plate. The whole assembly was then post-treated in a UV or thermal chamber. Assuming that both cured layers exhibit the same degree of resin polymerisation at the end of the curing/post-curing process and undergo the same thermal expansions, any warpage observed after the selected post-treatment process of the two-layer laminate is due to the additional polymerisation shrinkage that only the new half undergoes.

The out-of-plane deflection (warpage) of the SL formed resin plates was measured by means of projection or shadow moiré [9]. This method is ideal for obtaining full-field contour maps of large surfaces. A master grating is placed in front of the resin specimen and illuminated by a collimated light beam at an angle to the grating. The master grating and its shadow on the surface of the specimen then produces a fringe pattern viewed normally to the master grating. The out-of-plane displacement is given by

$$w = \frac{pn}{\tan \vartheta} \tag{1}$$

where p is the grating pitch, n the fringe order and ϑ the angle of incidence of the oblique light beam.

In the present work discussed here a grating of 0.56 pitch (18 lines/cm) was obtained in the form of transfer sheets. Transparent replicas of the grating were made and taped flat to a glass sheet. The sheet with the grating was held flat in front of the laminate specimen at a short distance from its surface. A 35 mm slide projector was used as a light source, illuminating the specimen at 45° to the normal of the grating. Fringe patterns were viewed normally to the grating and recorded with a digital camera. The experimental setup is shown in Fig. 1 while typical moiré fringe patterns are illustrated in Figs. 4–7. The fringes obtained represented loci of points of constant out-of-plane deflection such that all points on a given fringe corresponded to a deflection of one grating pitch relative to the points of the neighbouring fringe. The fringe patterns were analysed according to the theory described next. For a fringe pattern containing several elliptical contour fringes, the determination above can be made for various fringe orders (ellipses) to increase the accuracy.

3. Analysis of polymerisation shrinkage strains

The fabricated specimen plates were analysed as a laminate consisting of two parallel orthotropic layers, under plane stress, of equal thickness and equal thermal and

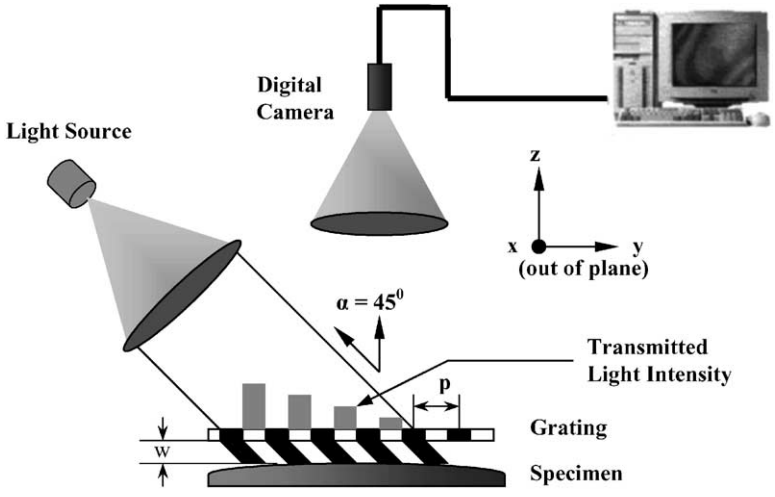

Fig. 1. Schematic representation of experimental setup for measuring out-of-plane deflections.

mechanical properties [10]. After subjecting the laminate plate to the second curing and post-curing process the chemical (or polymerisation) shrinkage strain in layer 1 is assumed to be zero:

$$\begin{bmatrix} e_x^c \\ e_y^c \\ e_{xy}^c \end{bmatrix}_1 = \begin{bmatrix} 0 \\ 0 \\ 0 \end{bmatrix} \tag{2}$$

The unrestrained chemical shrinkage strain in layer 2 would be

$$\begin{bmatrix} e_x^c \\ e_y^c \\ e_{xy}^c \end{bmatrix}_2 = \begin{bmatrix} e_1^c \\ e_2^c \\ 0 \end{bmatrix} \tag{3}$$

assuming that x- and y-axes coincide with the principal material axes, obtained along and perpendicular to the scan direction.

The shrinkage strains in the x- and y-axes of the model laminate are related to the laminate curvatures as follows [7]:

$$\frac{4h}{3}\begin{bmatrix} \kappa_1 \\ \kappa_2 \end{bmatrix} = \begin{bmatrix} e_1^c \\ e_2^c \end{bmatrix} \tag{4}$$

Integration of the curvature displacements relationships

$$\kappa_x = -\frac{\partial^2 w}{\partial x^2}, \qquad \kappa_y = -\frac{\partial^2 w}{\partial y^2}, \qquad \kappa_{xy} = -\frac{2\partial^2 w}{\partial x \partial y} \tag{5}$$

and ignoring rigid body displacements, we obtain for the out-of-plane deflection w at any point on a square laminate of side dimension a:

$$w(x,y) = -\tfrac{1}{2}(\kappa_x x^2 + \kappa_y y^2) \tag{6}$$

where κ_x and κ_y are the mid-plane curvatures of the laminate plate (Fig. 2). Thus, contours of equal deflection are ellipses as shown by the moiré fringe pattern. Each elliptical fringe corresponds to a deflection w_n.

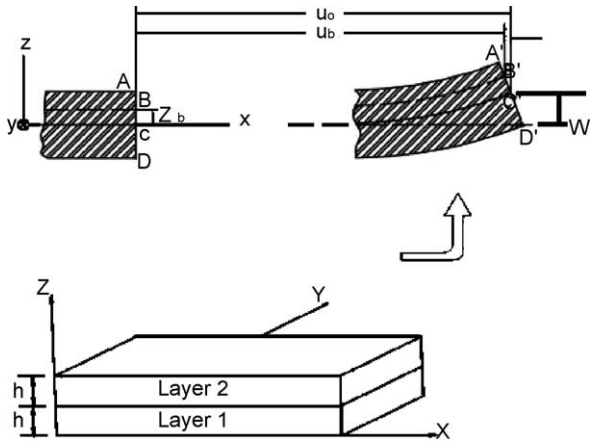

Fig. 2. Schematic diagram of two-layer resin laminate before and after deformation.

For an elliptical fringe with semi-axes a and b along the x- and y-axes and corresponding to a deflection w, it is obtained

$$\kappa_x = \kappa_1 = -\frac{2w}{a^2}, \qquad \kappa_y = \kappa_2 = -\frac{2w}{b^2} \tag{7}$$

Solving Eq. (4) for e_1^c and e_2^c we obtain

$$e_1^c = -\frac{8hw}{3a^2}, \qquad e_2^c = -\frac{8hw}{3b^2} \tag{8}$$

Thus, the components of chemical shrinkage determined by the method followed here are independent of the material properties of the layers, since they are the same for both layers.

4. Results and discussion

The fringe patterns illustrated were analysed by measuring the major and minor axes of the concentric elliptical fringes corresponding to integral fringe orders (dark fringes) and to integral plus one-half fringe orders (light fringes). These values (a and b) and the corresponding fringe order, n, were used in Eqs. (1) and (8) to obtain several sets of values for the polymerisation shrinkage strains, e_1^c and e_2^c, for the grating (ruling) used.

Laser curing of the second resin layer on top of the first layer resulted to significant out-of-plane deflection of the laminate plate as seen in Fig. 3. Projection moiré of the curved laminates gave fringe patterns consisting of concentric elliptical black and white lines (Figs. 4–7). Distinct differences were noted for the viewed fringe patterns before and after post-treatment. During post-curing of the two-layer laminate, the second layer shrinks additionally as it is further polymerised, leading to an increase of the exhibited out-of-plane deflection. Post-curing of the examined laminate plates under UV exposure resulted in the formation of circular fringes, indicating that the laminate plate shrinks proportionally along its plane directions. When post-curing took place in the thermal chamber the viewed patterns were of elliptical shape, exhibiting higher shrinkage in the y-axis. This observation leads to the conclusion that thermal post-curing results to more fully cured parts of higher distortion, which compares well with the findings of other researchers [11].

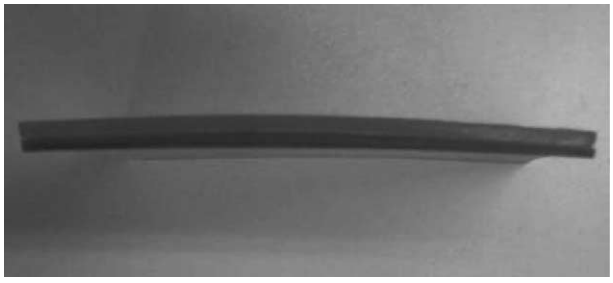

Fig. 3. Out-of-plane deformation of two-layer resin laminate.

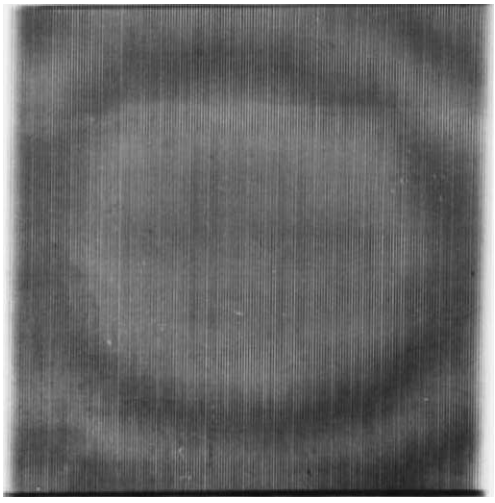

Fig. 4. Projection moiré pattern for two-layer resin laminate before UV post-curing (ruling of 18 lines/cm).

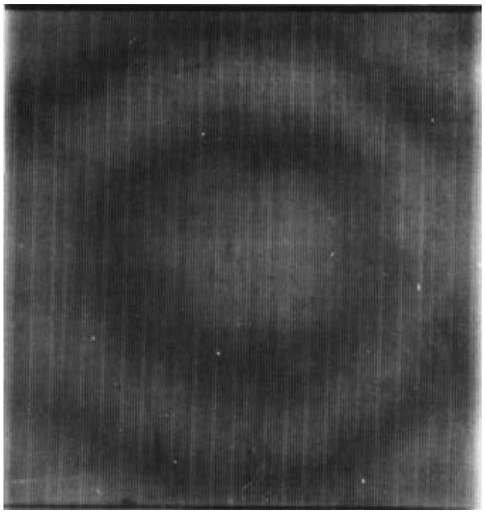

Fig. 5. Projection moiré pattern for two-layer resin laminate after UV post-curing (ruling of 18 lines/cm).

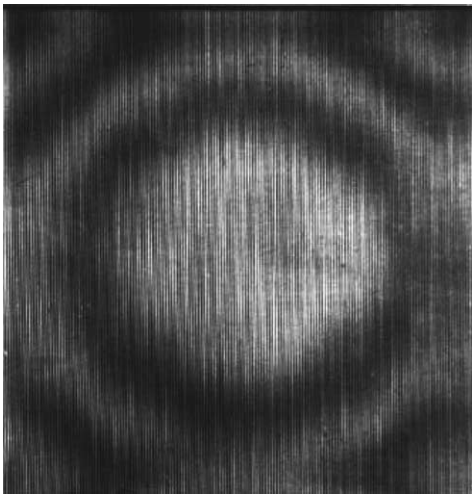

Fig. 6. Projection moiré pattern for two-layer resin laminate before thermal post-curing (ruling of 18 lines/cm).

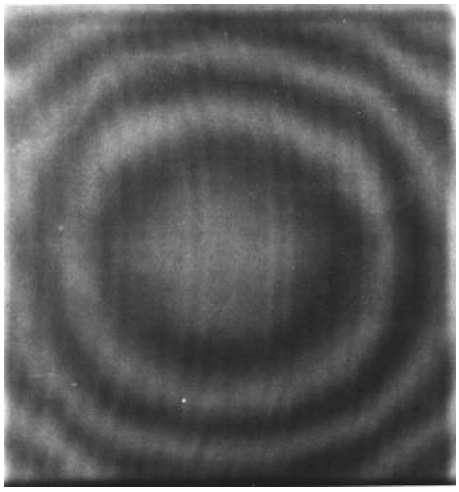

Fig. 7. Projection moiré pattern for two-layer resin laminate after thermal post-curing (ruling of 18 lines/cm).

Table 1
Measurement of polymerisation shrinkage strains

Post-treatment	Fringe order, n	a (mm)	b (mm)	$e_1^c \times 10^{-6}$	$e_2^c \times 10^{-6}$
UV	0.5	22	22	5091	5091
	1	33	33	4525	4525
	1.5	44	44	3818	3818
Average				4480	4480
Thermal	0.5	26	20	3645	6160
	1	32	26	4813	7290
	1.5	40	36	4620	5704
	2	46	40	4658	6160
Average				4434	6227

The analysis followed in the present work, based on the elastic lamination theory, could only be implemented for the determination of chemical shrinkage strains resulting after post-curing of the resin laminates, since only then would both layers exhibit the same mechanical properties. Typical results of measured shrinkage strains for the additionally polymerised test specimens are tabulated in Table 1.

5. Conclusions

An experimental investigation combined with a theoretical analysis based on elastic lamination theory was undertaken to determine the magnitude of the resulting shrinkage strains in a laser solidified acrylic-based photopolymer. Standard two-layer square samples were fabricated and subsequently subjected to UV and thermal post-treatment. The resulting warpage, consisting of elliptical equal deflection contours, was recorded experimentally using the shadow (or projection) moiré technique and correlated to the chemical shrinkage by means of lamination theory. It is concluded that that the simple experimental methodology

followed in this study could be implemented for the investigation of the shrinkage characteristics of photopolymer resins used in SL. The results shown in Table 1 demonstrate that both post-treatment processes lead to the generation of polymerisation shrinkage strains of considerable magnitude. It was also found that test specimens post-cured under intense UV light exhibited a uniform shrinkage, while thermal post-curing resulted to higher shrinkage strains. Finally, the same experimental setup and analysis technique could be readily applied in future studies concerning the investigation of polymerisation shrinkage strains in fibre reinforced SL parts of improved mechanical properties.

References

[1] P.F. Jacobs, Rapid Prototyping & Manufacturing—Fundamentals of Stereolithography, Society of Manufacturing Engineers, Dearborn, MI, 1992.
[2] G.A. Van Fo Fy, Theory of shrinkage stresses in oriented glass-reinforced plastics, Mechanika Polymerov 6 (1965) 61–68.
[3] J.Y.H. Fuh, L. Lu, C.C. Tan, Z.X. Shen, S. Chew, Curing characteristics of acrylic photopolymer used in stereolithography process, Rapid Prototyping J. 5/1 (1999) 27–34.
[4] J.Y.H. Fuh, L. Lu, C.C. Tan, Z.X. Shen, S. Chew, Processing and characterising photo-sensitive polymer in the stereolithography process, J. Mater. Process. Technol. 89–90 (1999) 211–217.
[5] K.-H. Dusel, J. Eschl, B. Wiedemann, Improvement of part accuracy—investigations into the basics of photopolymerization, in: Proceedings of the Fifth European Conference on Rapid Prototyping and Manufacturing, Helsinki, Finland, June 4–6, 1995.
[6] B. Harper, D. Peretz, Y. Weitsman, Assessment of chemical cure shrinkage stresses in two technical resins, in: Proceedings of the AIAA/ASME/ASCE/AHS 24th Structures, Structural Dynamics and Materials Conference, Lake Tahoe, Nevada, May 2–4, 1983.
[7] I.M. Daniel, T.-M. Wang, D. Karalekas, J.T. Gotro, Determination of chemical cure shrinkage in composite laminates, J. Comp. Technol. Res. 12/3 (1990) 172–176.
[8] D. Karalekas, I.M. Daniel, J.T. Gotro, in: S.A. Paipetis, G.C. Papanicolaou (Eds.), Phase Interaction in Composite Materials, Omega Scientific, London, 1988, pp. 574–584.
[9] W.J. Dally, F.W. Riley, Experimental Stress Analysis, McGraw-Hill, New York, 1992, p. 380.
[10] D. Karalekas, A proposed analysis and experimental methodology for the determination of cure shrinkage in SL formed plates, in: Proceedings of the Ninth European Conference on Rapid Prototyping and Manufacturing, Athens, Greece, July 17–19, 2000.
[11] J. Colton, B. Blair, Experimental study of post-build cure of stereolithography polymers for injection molds, Rapid Prototyping J. 5/2 (1999) 72–81.